Inorganic Chemistry

ARTICLE

pubs.acs.org/IC

Microwave-Assisted Construction of Ferromagnetic Coordination Polymers of $[W^V(CN)_8]^{3-}$ with Cu^{II}-pyrazole Synthons

Olaf Stefanczyk,*[,†] Tomasz Korzeniak,[†] Wojciech Nitek,[†] Michał Rams,[‡] and Barbara Sieklucka*[,†]

[†]Faculty of Chemistry, Jagiellonian University, Ingardena 3, 30-060 Kraków, Poland

[‡]M. Smoluchowski Institute of Physics, Jagiellonian University, Reymonta 4, 30-059 Kraków, Poland

Supporting Information

ABSTRACT: The microwave-mediated self-assembly of $[W^V(CN)_8]^{3-}$ with Cu^{II} in the presence of pyrazole ligand resulted in the formation of three novel assemblies: $Cu^{II}_2(Hpyr)_5(H_2O)[W^V(CN)_8](NO_3)\cdot H_2O$ (**1**), $\{Cu^{II}_5(Hpyr)_{18}[W^V(CN)_8]_4\}\cdot[Cu^{II}(Hpyr)_4(H_2O)_2]\cdot 9H_2O$ (**2**), and $Cu^{II}_4(Hpyr)_{10}(H_2O)[W^V(CN)_8]_2(HCOO)_2\cdot 4.5H_2O$ (**3**) (Hpyr =1H-pyrazole). Single-crystal X-ray structure of **1** consists of cyanido-bridged 1-D chains of vertex-sharing squares topology. The structure of **2** reveals 2-D hybrid inorganic layer topology with large coordination spaces occupied by $\{Cu(Hpyr)_2(H_2O)_4\}^{2+}$ ions. Compound **3** contains two types of cyanido-bridged 1-D chains of vertex-sharing squares linked together by formate ions in two directions forming hybrid inorganic−organic 3-D framework (I^1O^2). The magnetic measurements for **1**−**3** reveal a weak ferromagnetic coupling through Cu^{II}−NC−W^V bridges.

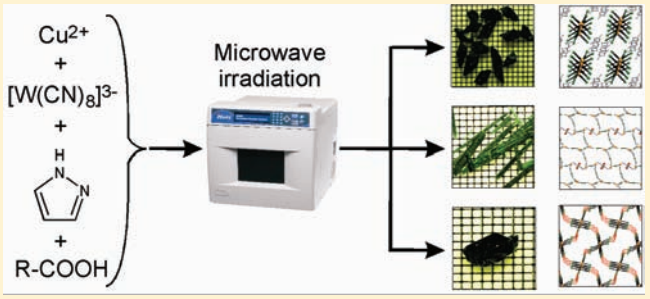

INTRODUCTION

The intensive attention paid to hybrid inorganic−organic materials reflects essential interest in their structural versatility and applications to gas sorption, ion-exchange, and catalysis.[1−3] The structural complexity of such materials, derived from the octacyanidometallate moiety, 3d metal center, and organic ligand provides the potential for the design of novel multifunctional materials.[1,4]

The coordination lability of the copper(II) complexes combined with the stereochemical nonrigidity of the $[M(CN)_8]^{n-}$ ions allows the formation of clusters,[5] discrete molecules,[6,7] 1-D chains,[8−10] 2-D layers,[11−25] and 3-D networks.[20,26−33] The majority of Cu^{II}−NC−W^V systems display ferromagnetic coupling between metal centers,[5−8,10,12,15,17,19−31] and metamagnetism was observed in some materials.[11,13,14,16] Introduction of organic ligand to Cu^{II}−$[W^V(CN)_8]^{3-}$ systems provides the rational pathway for modification of their structure and magnetic properties.

The polyazaheteroaromatic pyrazole ligand is the potentially attractive organic component of Cu^{II}−$[W^V(CN)_8]^{3-}$ systems in view of documented ability to bridge Cu(II) ions to form polynuclear compounds. The pyrazole bridges were observed in the trinuclear copper(II) complexes $[Cu_3(OH)(pyr)_3(HCOO)_2(Hpyr)_2]$[34] and $[Cu_3(OH)(pyr)_3(Hpyr)_2Cl_2]\cdot$solv (solv = H_2O, tetrahydrofuran)[35] and 1-D chains $[Cu^{II}(pyr)_2\cdot solv]_n$ (solv = H_2O, NH_3, $MeNH_2$, MeCN, pyridine, MeOH, EtOH).[36] The characteristic feature of polynuclear Cu(II) assemblies with pyrazole is the presence of $[Cu^{II}(Hpyr)_2(H_2O)_4]^{2+}$ and $[Cu^{II}(Hpyr)_4(H_2O)_2]^{2+}$ synthons. Moreover, pyrazole molecules act as the terminal ligands and form copper(II) mononuclear complexes $[Cu^{II}(Hpyr)_6]X_2$ (X= ClO_4^-, AsF_6^-, PF_6^-),[37] $[Cu^{II}(Hpyr)_4Cl_2]$,[38,39] and $[Cu^{II}(Hpyr)_2Cl_2]\cdot H_2O$,[39] and 1-D chains $[Cu^{II}(Hpyr)_4SO_4](H_2O)$.[40] Additionally, the cations H_2pyr^+ have been found in pyrazolium salt $[H_2pz]_2[CuCl_4]$.[41]

As a part of our investigations of the structural diversity and the magnetic properties of Cu^{II}−$[W^V(CN)_8]^{3-}$ assemblies we have prepared a series of Hpyr−Cu^{II}−$[W^V(CN)_8]^{3-}$ coordination networks. We decided to investigate for the first time the effect of microwave radiation on the process of formation of Cu^{II}−$[W^V(CN)_8]^{3-}$ systems. The results of our experiments involving microwave-aided self-assembly consist of three new coordination polymers $Cu^{II}_2(Hpyr)_5(H_2O)[W^V(CN)_8](NO_3)\cdot H_2O$ (**1**), $\{Cu^{II}_5(Hpyr)_{18}[W^V(CN)_8]_4\}\cdot[Cu^{II}(Hpyr)_4(H_2O)_2]\cdot 9H_2O$ (**2**), and $Cu^{II}_4(Hpyr)_{10}(H_2O)[W^V(CN)_8]_2(HCOO)_2\cdot 4.5H_2O$ (**3**).

Structures of these compounds were solved using single-crystal X-ray diffraction. The magnetic properties reveal the interplay of weak ferro- and antiferromagnetic interactions due to the presence of different coordination environment of paramagnetic metal centers in the coordination networks of I^1O^0, I^2O^0, and I^1O^2 for **1**, **2**, and **3**, respectively.

EXPERIMENTAL SECTION

Materials. Pyrazole and 85% HCOOH were purchased from commercial sources (Sigma-Aldrich, POCh) and used as received.

Received: April 5, 2011
Published: August 19, 2011

Table 1. Crystal Data, Data Collection, and Refine Parameters for 1−3

	1	2	3
molecular formula	$C_{23}H_{24}Cu_2N_{19}O_5W$	$C_{49}H_{55}Cu_3N_{38}O_{5.5}W_2$	$C_{96}H_{106}Cu_8N_{72}O_{19}W_4$
M_r	957.54	1822.20	3815.44
T (K)	293(2)	293(2)	293(2)
radiation used, λ (Å)	Mo Kα (0.710 73)	Mo Kα (0.710 73)	Mo Kα (0.710 73)
cryst system	monoclinic	triclinic	triclinic
space group	$C2/c$	$P\bar{1}$	$P\bar{1}$
a (Å)	31.0150(6)	11.8120(2)	14.7530(2)
b (Å)	14.6360(3)	14.7920(3)	16.5290(2)
c (Å)	15.4030(3)	21.6160(4)	16.6930(3)
α (deg)	90	70.8300(10)	61.9300(10)
β (deg)	90.5050(10)	82.2460(10)	87.2970(10)
γ (deg)	90	82.4880(10)	87.6650(10)
V (Å^3)	6991.7(2)	3519.66(11)	3587.02(9)
Z	8	2	1
d_{calcd} (g cm^{-3})	1.819	1.719	1.766
μ (mm^{-1})	4.551	4.220	4.434
F(000)	3736	1787	1865
crystal size (mm^3)	0.40 × 0.20 × 0.15	0.35 × 0.08 × 0.04	0.30 × 0.30 × 0.25
θ range for data collection (deg)	2.94−27.48	2.69−27.42	1.38−27.48
index ranges	$-38 \le h \le 40$	$-15 \le h \le 15$	$-19 \le h \le 19$
	$-19 \le k \le 18$	$-17 \le k \le 19$	$-21 \le k \le 21$
	$-19 \le l \le 19$	$-27 \le l \le 27$	$-19 \le l \le 21$
reflns collected	28 629	26 592	28 457
indep reflns	7991	15 713	16 288
	[R(int) = 0.0358]	[R(int) = 0.0308]	[R(int) = 0.0319]
completeness of θ (%)	99.7 (θ = 27.48°)	98.0 (θ = 27.42°)	98.9 (θ = 27.48°)
max/min transmission	0.5485/0.2633	0.8494/0.3198	0.4036/0.3497
refinement method	full-matrix least-squares on F^2	full-matrix least-squares on F^2	full-matrix least-squares on F^2
data/restraints/params	7991/0/452	15 713/0/889	16 288/0/896
GOF on F^2	1.058	0.988	1.066
final R indices ($I > 2\sigma(I)$)	R1 = 0.0296, wR2 = 0.0710	R1 = 0.0352, wR2 = 0.0730	R1 = 0.0377, wR2 = 0.0951
R indices (all data)	R1 = 0.0415, wR2 = 0.0755	R1 = 0.0602, wR2 = 0.0793	R1 = 0.0512, wR2 = 0.1016
largest diff. peak and hole (e Å^{-3})	1.724 and −1.006	1.831 and −1.131	3.245 and −1.635

Octacyanidotungstate(V) sodium[42] and cesium[43] salts have been synthesized according to the published procedures.

Synthesis of $Cu^{II}_2(Hpyr)_5(H_2O)[W^V(CN)_8](NO_3)\cdot H_2O$ (1). Microwave syntheses were performed in MARS 240/50 (CEM Corp.) with the use of a GlassChem 20 vessel set. To a solution containing $Cu(NO_3)\cdot 3H_2O$ (0.242 g, 1 mmol, 8 mL of H_2O) and HCOOH (76 μL, 1.7 mmol) was added a solution of pyrazole (0.204 g, 3 mmol, 8 mL of H_2O), followed by an immediate addition of a solution containing $Na_3[W(CN)_8]\cdot 4H_2O$ (0.352 g, 0.66 mmol, 8 mL of H_2O) upon vigorous stirring. Green precipitate formed immediately. Then, the reaction mixture was irradiated to a maximum reaction temperature of 110 °C for 5 min and gradually cooled down to room temperature for 1 h. The resulting solution was filtered and left in the dark in a closed vessel at room temperature. After a few hours green needles were formed, which recrystallized over 3 weeks forming green single crystals of **1**. Yield: 176 mg (36.8%). Elementary Anal. Calcd for $C_{23}H_{23}Cu_2N_{19}O_5W$ (**1**): C, 28.85%; H, 2.53%, N, 27.79%. Found: C, 29.08%; H, 2.58%; N, 27.66%. IR spectrum in ν(CN) region (cm^{-1}): 2202 m, 2183 m (Supporting Information, Table S1).

Synthesis of $\{Cu^{II}_5(Hpyr)_{18}[W^V(CN)_8]_4\}\cdot[Cu^{II}(Hpyr)_4(H_2O)_2]\cdot 9H_2O$ (2). An analogous microwave-mediated procedure to that of **1** was applied, but copper(II) sulfate and acetic acid were used instead of copper(II) nitrate and formic acid. The dark green single crystals were formed through recrystallization of the precipitate obtained from the resulting solution. Yield: 146 mg (29.4%). Elementary Anal. Calcd for $C_{98}H_{114}Cu_6N_{76}O_{13}W_4$ (**2**·$2H_2O$): C, 31.98%; H, 3.12%; N, 28.62%. Found: C, 31.97%; H, 3.07%; N, 28.67%. IR spectrum in ν(CN) region (cm^{-1}): 2145 m (Supporting Information, Table S1).

Synthesis of $Cu^{II}_4(Hpyr)_{10}(H_2O)[W^V(CN)_8]_2(HCOO)_2\cdot 4.5H_2O$ (3). This assembly was obtained similarly to **1**, but copper sulfate instead of copper nitrate was used. In the microwave-assisted synthesis HCOOH was used, resulting in green single crystals of **3** formed through recrystallization within 2 weeks. Yield: 150 mg (31.5%). Elementary Anal. Calcd for $C_{48}H_{54}Cu_4N_{36}O_{10}W_2$ (**3**·$0.5H_2O$): C, 30.07%; H, 2.84%; N, 26.30%. Found: C, 30.14%; H, 2.78%; N, 26.23%. IR spectrum in ν(CN) region (cm^{-1}): 2203 m, 2181 m (Supporting Information, Table S1).

In the all syntheses, green precipitate has been identified as the identical primary product $Cu^{II}_3(Hpyr)_6[W^V(CN)_8]_2\cdot 3.5H_2O$ (**A**). Elementary Anal. Calcd for $C_{34}H_{31}Cu_3N_{28}O_{3.5}W_2$: C, 28.24%; H, 2.16%; N, 27.12%. Found: C, 28.34%; H, 1.85%; N, 27.02%. IR spectrum in ν(CN) region (cm^{-1}): 2192 m, 2167 m(sh), 2147 m (Supporting Information, Table S1). All attempts to obtain single crystals of **A** suitable for X-ray diffraction analysis were unsuccessful.

X-ray Crystallography. The single-crystal diffraction data for all three structures were collected using the Nonius Kappa CCD equipped

dx.doi.org/10.1021/ic200689a |*Inorg. Chem.* 2011, 50, 8808–8816

Table 2. Selected Bond Lengths (Å) and Bond Angles (deg) for 1−3

1				2				3			
Cu2−N11	2.002(3)	Cu2−N11−C11	175.0(4)	Cu3−N11	2.375(4)	Cu3−N11−C11	160.9(4)	Cu3−N14	2.324(4)	Cu3−N14−C14	168.2(4)
Cu2−N16	2.188(3)	Cu2−N16−C16	178.5(4)	Cu4−N15	2.531(4)	Cu4−N15−C15	157.1(4)	Cu3−N18	2.004(4)	Cu3−N18−C18	176.1(4)
Cu3−N13	2.201(4)	Cu3−N13−C13	176.3(4)	Cu5−N14	2.669(4)	Cu5−N14−C14	149.7(4)	Cu3−O633	2.616(5)	Cu3−O633−C632	129.3(5)
Cu3−N18	2.017(3)	Cu3−N18−C18	175.9(3)	Cu5−N25	2.570(4)	Cu5−N25−C25	152.5(4)	Cu4−N24	2.008(4)	Cu4−N24−C24	173.9(4)
W−C_{min}	2.155(4)	W−C−N_{min}	177.0(4)	Cu6−N26	2.389(4)	Cu6−N26−C26	165.6(4)	Cu4−N28	2.293(5)	Cu4−N28−C28	162.9(4)
W−C_{max}	2.173(4)	W−C−N_{max}	179.3(4)	W−C_{min}	2.148(5)	W−C−N_{min}	176.4(4)	Cu4−O431	1.986(4)	Cu4−O431−C432	130.8(4)
W−C_{av}	2.166(4)	W−C−N_{av}	178.4(4)	W−C_{max}	2.178(5)	W−C−N_{max}	178.9(4)	Cu5−N12	1.998(5)	Cu5−N12−C12	170.3(4)
W1−^{C11N11}−Cu2	5.297[a]	C11−W1−C16	72.15(15)	W−C_{av}	2.167(5)	W−C−N_{av}	177.3(4)	Cu5−N16	2.267(4)	Cu5−N16−C16	168.9(5)
W1−^{C16N16}−Cu2	5.487[a]	C13−W1−C18	72.90(15)	W1−^{C11N11}−Cu3	5.577[a]	C11−W1−C14	74.63(16)	Cu5−O433	2.724[a]	Cu5−O433−C432	141.6[a]
W1−^{C13N13}−Cu3	5.512[a]	N11−Cu2−N16	107.73(15)	W1−^{C15N15}−Cu4	5.704[a]	C11−W1−C15	81.18(16)	Cu6−N22	2.034(4)	Cu6−N22−C22	174.9(5)
W1−^{C18N18}−Cu3	5.324[a]	N13−Cu3−N18	102.66(15)	W1−^{C14N14}−Cu5	5.752[a]	C14−W1−C15	142.67(15)	Cu6−N26	2.160(4)	Cu6−N26−C26	168.9(5)
				W2−^{C25N25}−Cu5	5.697[a]	C25−W2−C26	75.09(16)	Cu6−O631	1.971(4)	Cu6−O631−C632	122.7(4)
				W2−^{C26N26}−Cu6	5.642[a]			W−C_{min}	2.150(5)	W−C−N_{min}	175.3(4)
								W−C_{max}	2.179(5)	W−C−N_{max}	179.8(5)
								W−C_{av}	2.167(5)	W−C−N_{av}	178.3(5)
								W1−^{C14N14}−Cu3	5.599[a]	C12−W1−C16	74.67 (18)
								W1−^{C18N18}−Cu3	5.299[a]	C14−W1−C18	75.08(18)
								W1−^{C12N12}−Cu5	5.267[a]	C22−W2−C26	74.1(2)
								W1−^{C16N16}−Cu5	5.543[a]	C24−W2−C28	74.51(18)
								W2−^{C24N24}−Cu4	5.311[a]	N14−Cu3−N18	93.43(17)
								W2−^{C28N28}−Cu4	5.512[a]	N24−Cu4−N28	91.86(18)
								W2−^{C22N22}−Cu6	5.328[a]	N12−Cu5−N16	94.40(18)
								W2−^{C26N26}−Cu6	5.435[a]	N22−Cu6−N26	101.3(2)
								Cu3−$^{O(CH)O}$−Cu6	6.217[a]		
								Cu4−$^{O(CH)O}$−Cu5	6.095[a]		

[a] The metric parameters calculated with the use of the CCDC Mercury visualization software.[48]

dx.doi.org/10.1021/ic200689a |Inorg. Chem. 2011, 50, 8808–8816

Scheme 1. Microwave Synthesis Scheme of 1−3

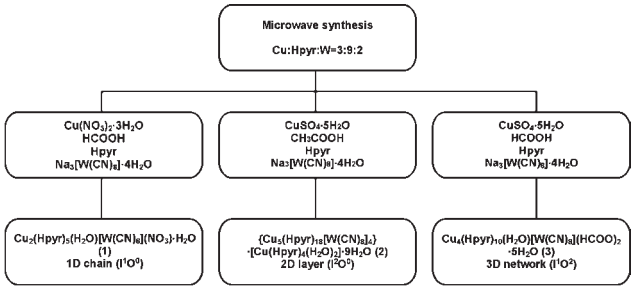

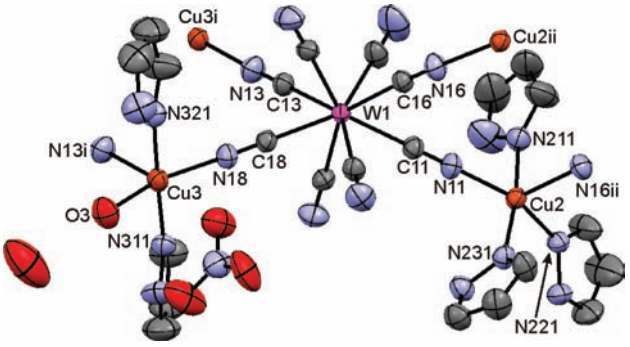

Figure 1. ORTEP diagram of structure unit of **1** with selected atoms labeling. Hydrogen atoms were removed for clarity. Colors used: Cu, orange; N, blue; C, gray; W, magenta, O, red. Symmetry codes: i = 0.5 − *x*, 0.5 − *y*, 1 − *z*; ii = −*x*, *y*, 1.5 − *z*. Thermal ellipsoids of 50% probability are shown.

with a Mo Kα radiation source (λ = 0.710 73 Å) and graphite monochromator. In each case the procedure of the structure solution and refinement was very similar. The space group was determined using the ABSEN.[44] Structure was solved by direct methods using SIR-97.[45] Refinement and further calculations were carried out using the SHELXL-97[46] package incorporated in WinGX 1.64 crystallographic collective package.[47] The non-H atoms with the exception of the atom O6 in **3** were refined anisotropically using weighted full-matrix least-squares on F^2. The attempts to refine the mentioned atom anisotropically gave the nonpositive definite. All hydrogen atoms joined to carbon and nitrogen atoms of organic component of the compound **1** were positioned with an idealized geometry and refined using a riding model with $U_{iso(H)}$ fixed at $1.2U_{eq(C)}$. Hydrogen atoms of crystallization and coordination water molecules were unreachable, so their positions were calculated at positions optimized to form the hydrogen bonds and refined using a riding model with $U_{iso(H)}$ fixed at $1.5U_{eq(C)}$. Crystal data, data collection, and refine parameters for **1**−**3** were listed in Table 1, and selected bond lengths and bond angles were presented in Table 2.

Physical Techniques. Infrared spectra were recorded in KBr pellets in range 4000−400 cm^{-1} using a Bruker EQUINOX 55 FT-IR spectrometer. Elemental analyses (C, H, N) were performed on an ELEMENTAR Vario Micro Cube CHNS instrument. Magnetic measurements were performed using a Quantum Design SQUID magnetometer MPMS5-XL. The thermal dependence of the magnetic susceptibility was measured at H_{dc} field of 1 kOe in temperature range 2−300 K. The field dependence of magnetization was measured in the 0−50 kOe magnetic field range. The structural data presented as figures were prepared with the use of the CCDC Mercury visualization software.[48] Geometries of metal centers were estimated with the Continuous Shape Measures (CShM) analysis with the use of SHAPE v2.0 software.[49]

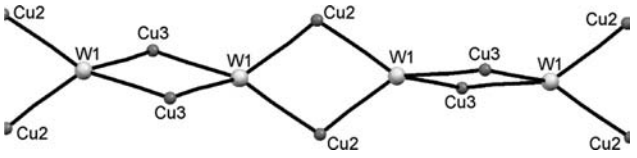

Figure 2. Chain structure of **1** with selected atoms labeling. Only metal centers and bridging atoms are shown.

RESULTS AND DISCUSSION

Syntheses. Microwave approach provides controlled heating conditions of the reactant solutions of Cu^{2+}, Hpyr, and $[W(CN)_8]^{3-}$ and leads to the formation of three new products. The synthesis with Cu/Hpyr/$[W(CN)_8]^{3-}$ = 3/9/2 ratio at ambient conditions results in the formation of primary green solid $Cu^{II}_3(Hpyr)_6[W^V(CN)_8]_2\cdot 3.5H_2O$ (**A**) only, regardless of the nature of Cu^{2+} salt and acid. The microwave synthesis with Cu/Hpyr/$[W(CN)_8]^{3-}$ = 3/9/2 ratio and use of copper(II) nitrate salt in presence of formic acid resulted in $Cu^{II}_2(Hpyr)_5(H_2O)[W^V(CN)_8](NO_3)\cdot H_2O$ (**1**). The use of copper(II) sulfate in presence of acetic acid afforded $\{Cu^{II}_5(Hpyr)_{18}[W^V(CN)_8]_4\}\cdot[Cu^{II}(Hpyr)_4(H_2O)_2]\cdot 9H_2O$ (**2**), while application of formic acid gave $Cu^{II}_4(Hpyr)_{10}(H_2O)[W^V(CN)_8]_2(HCOO)_2\cdot 4.5H_2O$ (**3**). In all microwave-assisted procedures we have observed the initial formation of the green precipitate, followed by topochemical reaction, where the green product (**A**) reversible changes to **1**, **2**, or **3** in the presence of specific anion (Scheme 1). Products **1**−**3** could be obtained in microwave-assisted synthesis only. Conventional heating of the each reaction mixture, contrary to microwave irradiation, results in reduction of octacyanidotungstate(V) to octacyanidotungstate(IV) and partial release of CN^- ligands.

Single-Crystal X-ray Structure of 1. The crystal structure of **1** (Figure 1) consists of $[Cu^{II}(H_2O)(Hpyr)_2]^{2+}$ and $[Cu^{II}(Hpyr)_3]^{2+}$ units bridged by $[W^V(CN)_8]^{3-}$, nitrate anions, and crystallization water molecules. The bridging between metal centers leads to formation of a 1-D chain of vertex-sharing $Cu^{II}_2W^V_2$ squares topology (Figure 2). The squares are twisted relative to each other by the angle close to 70°. The molecular structure of the assembly can be classified as an inorganic hybrid chain (I^1O^0) according to Cheetham.[1] Octacyanidotungstate(V) ion reveals distorted dodecahedral (DD-8) geometry (Supporting Information, Table S2). The bond lengths and angles (Table 2) reveal typical values for systems based on octacyanidotungstates.[50] Four cyanido ligands of $[W^V(CN)_8]^{3-}$ are bridging two Cu2 (C11−N11 and C16−N16) as well as two Cu3 centers (C13−N13 and C18−N18). The $[Cu2(Hpyr)_3(NC)_2]$ unit reveals square pyramidal (SPY-5) geometry with one axial and one equatorial cyanido-bridge (Supporting Information, Table S3). The axial bridge is relatively longer with Cu2−N16 bond length of 2.188(4) Å compared to the equatorial Cu2−N11 linkage of 2.002(3) Å length. Both bridges are almost linear revealing Cu−N−C angles of 178.5(4)° and 175.0(4)° for Cu2−N16−C16 and Cu2−N11−C11, respectively. The coordination sphere of Cu2 is completed by three nitrogen atoms from pyrazole ligands with the average Cu2−N distance of 2.012(3) Å. The coordination geometry of the $[Cu3(H_2O)(Hpyr)_2(NC)_2]$ represents square pyramidal (SPY-5) geometry. The cyanido-bridges Cu3−N13 and Cu3−N18 coordinate in axial and equatorial positions, respectively. Similarly to the Cu2 coordination environment, both cyanido linkages are almost linear with the Cu3−N13−C13 and Cu3−N18−C18 angles of 176.3(4)° and 175.9(3)°, respectively. The axial bridge Cu3−N13 is significantly longer at

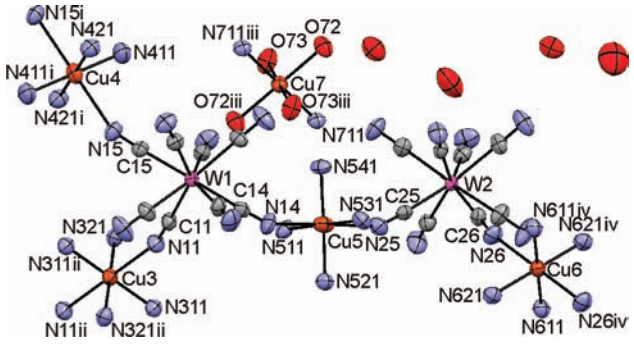

Figure 3. ORTEP diagram of structure unit of **2** with selected atoms labeling. Hydrogen atoms and noncoordinating atoms of pyrazole ligands are removed for clarity. Colors used: Cu, orange; N, blue; C, gray; W, magenta; O, red. Symmetry codes: i = −*x*, 1 − *y*, 2 − *z*; ii = −*x*, −*y*, 2 − *z*; iii = −*x*, 1 − *y*, 1− *z*; iv = 2 − *x*, −*y*, 1 − *z*. Thermal ellipsoids of 50% probability are shown.

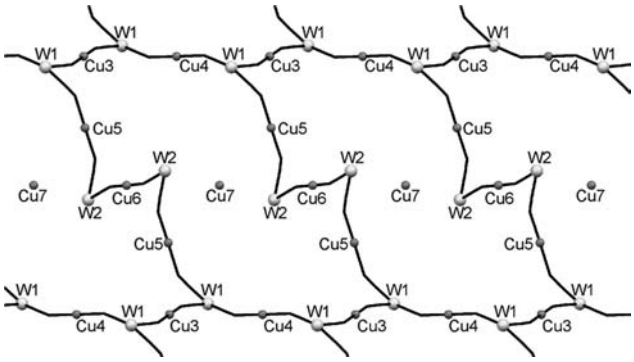

Figure 4. Layer frame of **2** in crystallographic direction (100).

2.201(4) Å in comparison to the equatorial Cu3−N18 linkage with the bond length of 2.017(3) Å. The nitrogen atoms from two pyrazole molecules and the oxygen donor from the water ligand form coordination bonds toward Cu3 with the average length of 1.995(3) Å. Water molecules and nitrate anions are stabilized within the molecular structure by the network of H-bonding incorporating also nitrogen atoms of terminal cyanido ligands and pyrazole molecules.

Single-Crystal X-ray Structure of 2. The crystal structure of **2** (Figure 3) consists of four $[Cu_i^{II}(Hpyr)_4]^{2+}$ (Cu_i = Cu3, Cu4, Cu5, Cu6) units bridged by two structurally different $[W^V(CN)_8]^{3-}$ ions forming a 2-D cyanido-bridged structure built of large 20-metallic grid and belongs to the hybrid inorganic layers (I^2O^0), according to Cheetham[1] (Figure 4). The $[Cu7^{II}(Hpyr)_2(H_2O)_4]^{2+}$ ion is located within the grid neutralizing the negative charge of the layer. The geometry of both octacyanidotungstate(V) ions reveals square antiprism (SAPR-8) coordination environment with a minor dodecahedral (DD-8) contribution (Supporting Information, Table S2). Three cyanide ligands of $[W1^V(CN)_8]^{3-}$ are bridging to Cu3 *via* C11−N11, Cu4 *via* C15−N15, and Cu5 *via* C14−N14, while $[W2^V(CN)_8]^{3-}$ are bridging to Cu5 *via* C25−N25 and Cu6 *via* C26−N26. The W−C and C−N bond lengths range from 2.148(5) to 2.178(5) Å and 1.130(5) to 1.152(6) Å, respectively (Table 2). All of the W−C−N linkages are almost linear with the W−C−N angles ranging from 176.4(4)° to 178.9(4)°, which is typical for systems based on octacyanidometallates.[50] The $[Cu(Hpyr)_4(NC)_2]$ units exhibit distorted octahedral geometry (OC-6) with strong tetragonal

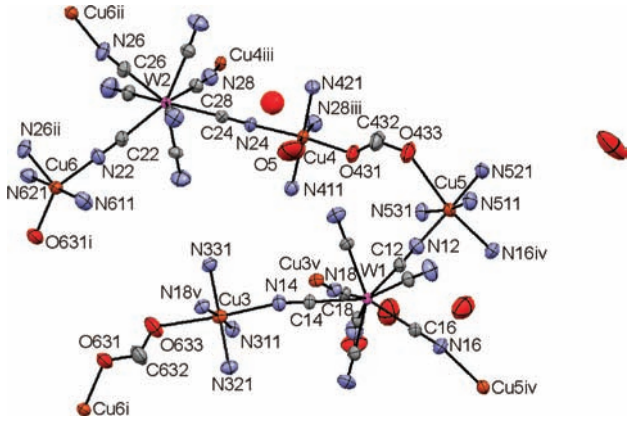

Figure 5. ORTEP diagram of structure unit of **3** with selected atoms labeling. Hydrogen atoms and noncoordinating atoms of pyrazole ligands are removed for clarity. Colors used: Cu, orange; N, blue; C, gray; W, magenta; O, red. Symmetry codes: i = 1 − *x*, 1 − *y*, −1 − *z*; ii = −*x*, 1 − *y*, −1 − *z*; iii = −*x*, 1 − *y*, −*z*; iv = 1 − *x*, −*y*, 1 − *z*; v = 1 − *x*, −*y*, −*z*. Thermal ellipsoids of 50% probability are shown.

elongation (Supporting Information, Table S3). In the case of Cu3−Cu6 metal centers the pyrazole ligands coordinate in the equatorial plane with Cu−N bonds of 1.988(4)−2.036(4) Å range. The axial positions are occupied by N atoms of cyanido-bridges characterized by Cu−N bond lengths between 2.375(4) and 2.669(4) Å, whereas the Cu−N−C angles fall within the range 149.7(4)−165.6(4)°, which indicates relatively weak bonding. The $[Cu7(Hpyr)_2(H_2O)_4]^{2+}$ ion exhibits distorted octahedral (OC-6) geometry with tetragonal elongation. The axial positions are coordinated by oxygen atoms of two water molecules with Cu7−O73 distance 2.422(4) Å, while the equatorial positions are occupied by two oxygen atoms of water molecules and two nitrogen atoms of pyrazole molecules with the average length of coordination bond in the equatorial position of 1.990(4) Å. The network of hydrogen bonding interactions involves water molecules and nitrogen atoms of terminal CN^-.

Single-Crystal X-ray Structure of 3. The crystal structure of **3** (Figure 5) reveals a 3-D inorganic−organic network built of cyanido- and formato-bridging ligands. The cyanido ligands bridge the metal centers allowing formation of two structurally different types of 1-D chains of vertex-sharing squares (Figure 6), which are twisted by the angle near 70°. The oxygen donors of formate anions coordinate two Cu centers from different chains, extending the connectivity into the 3-D network (Figure 7). Compound **3** belongs to the mixed inorganic−organic 3-D frameworks (I^1O^2), according to Cheetham.[1] The coordination geometries of both $[W1(CN)_8]^{3-}$ and $[W2(CN)_8]^{3-}$ moieties reveal distorted square antiprism (SAPR-8) geometry (Supporting Information, Table S2) with the metric parameters typical for this class of systems.[50] Each of the octacyanidotungstate ions reveals four bridging cyanido ligands toward copper centers forming two distinct chains, containing W1, Cu3, Cu5, and W2, Cu4, Cu6, respectively. The coordination sphere of $[Cu3(Hpyr)_3(NC)_2(HCOO)]$ displays the distorted octahedral (OC-6) geometry with strong tetragonal elongation (Supporting Information, Table S3). The equatorial positions are occupied by three nitrogen donors from pyrazole ligands and one cyanido-bridge Cu3−N18. The bond lengths fall within the range 1.996(4)−2.013(4) Å with Cu3−N18 bond length of 2.004(4) Å (Table 2). The coordination bonds in axial positions are significantly longer, revealing Cu3−N14

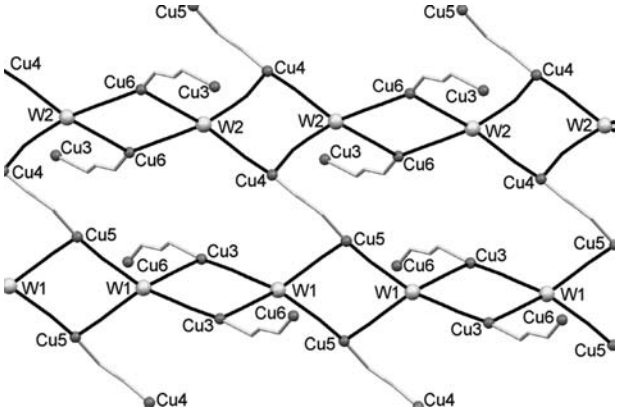

Figure 6. Chain structure of **3** with selected atoms labeling. Only metal centers and bridging atoms are shown. Colors used: CN^-, black; $HCOO^-$, light gray.

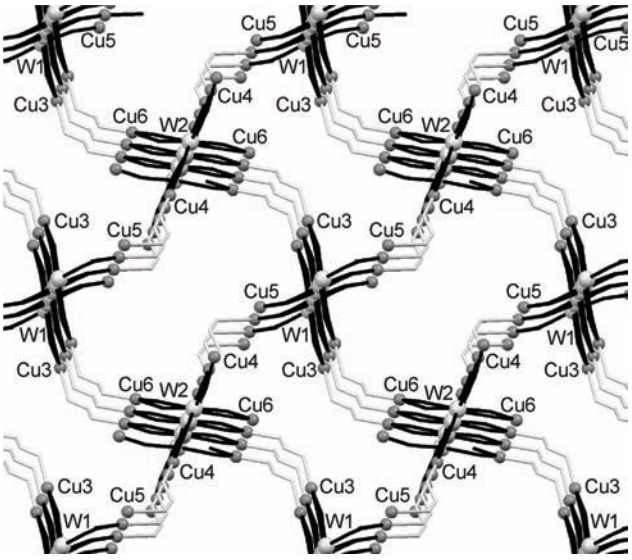

Figure 7. Chains frame of **3**. View on (001) direction. Colors used: CN^-, black; $HCOO^-$, light gray.

cyanido-bridge of 2.324(4) Å and Cu3−O633 formato-bridge of 2.616(5) Å. The axial bridge is more bent, displaying the Cu3−N14−C14 angle of 168.2(4)° compared to the value for the equatorial Cu3−N18−C18 linkage of 176.1(4)°. The similar coordination geometry and metric parameters are revealed in the $[Cu5(Hpyr)_3(NC)_2(HCOO)]$ moiety. The equatorial positions are occupied by three nitrogen donors from pyrazole ligands and one cyanido-bridge Cu5−N12 with the bond lengths range 1.984(5)−2.014(4) Å. The equatorial cyanido-bridge Cu5−N12 reveals bond length of 1.998(5) Å and Cu5−N12−C12 angle of 170.3(4)°. The axial sites are coordinated by one cyanido and one formato ligands forming bridges toward W1 and Cu4. The axial Cu5−N16 cyanido-bridge of 2.267(4) Å is slightly shorter than the Cu3−N14 bridge; however, the Cu5−O433 formato-bridge of 2.724 Å is notably longer than the corresponding Cu3−O633 bridge. The tetragonal elongation is even more pronounced in the coordination sphere of $[Cu4(H_2O)(Hpyr)_2(NC)_2(HCOO)]$, where the equatorial positions are occupied by two N donors from the pyrazole ligands and the N24 cyanido-bridge as well as the oxygen atom from the formato ligand. The bond lengths display values of 2.008(4) and

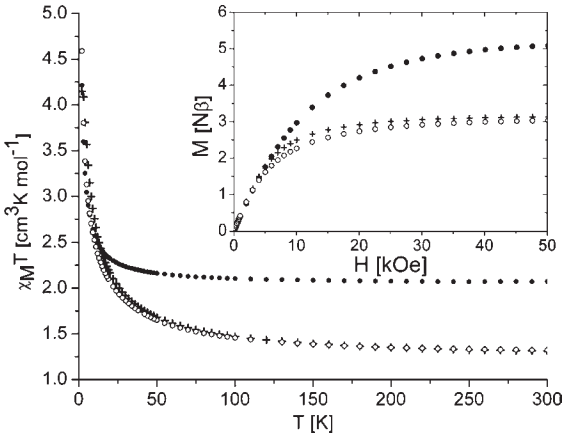

Figure 8. Thermal dependence of $\chi_M T$ for **1** (+), **2** (●), and **3** (○). Inset: field dependence of magnetization for **1** (+), **2** (●), and **3** (○).

1.986(4) Å for Cu4−N24 and Cu4−O431, respectively. The axial positions are coordinated by the N28 atom from cyanido ligand with Cu4−N28 bond length of 2.293(5) Å and the O5 water molecule with Cu4−O5 bond length of 2.774 Å. The $[Cu6(Hpyr)_2(NC)_2(HCOO)]$ reveals geometry of strongly distorted trigonal bipyramide (TBPY-5). Cyanido- and formato-bridges coordinate in the equatorial positions with bond lengths of 2.034(4), 2.160(4), and 1.971(4) Å for Cu6−N22, Cu6−N26, and Cu6−O631, respectively. The axial positions are coordinated by N donors from the pyrazole ligands with bond lengths of Cu6−N611 and Cu6−N621 of 1.978(5) and 2.003(5) Å, respectively. The enhanced connectivity between metal centers due to the formato-bridging allows connecting the 1-D cyanido-bridged chains into the 3-D inorganic−organic hybrid network structure; however, some of the Cu−$O_{formato}$ bonds are significantly longer than the typical coordination bonds[34,51] but below the limit of semicoordination bonds (3.07 Å).[52] The H-bonds stabilize the structure due to interactions between water molecules and nitrogen atoms of terminal CN^-.

Magnetic Properties. The magnetic data for **1**−**3** indicate the weak ferromagnetic interactions in these systems (Figure 8). The $\chi_M T$ values at room temperature for **1** and **3** reveal values of 1.31 and 1.32 cm^3 K mol^{-1}, respectively, which is consistent with the Curie value of 1.28 cm^3 K mol^{-1} for the value for three noninteracting spins $S = {}^1/_2$ (assuming $g_{Cu(II)} = 2.2$ and $g_{W(V)} = 2.0$). The experimental $\chi_M T$ for **2** of 2.07 cm^3 K mol^{-1} corresponds to the value for five noninteracting spins $S = {}^1/_2$ (assuming $g_{Cu(II)} = 2.17$ and $g_{W(V)} = 2.0$).

As temperature decreases the $\chi_M T$ values for **1**−**3** monotonously increase, and the paramagnetic Curie−Weiss temperatures (θ) estimated from data above 150 K are 17(1), 2(1), and 13(1) K for **1**, **2**, and **3**, respectively. No signs of long-range magnetic ordering were observed down to 2 K in all the compounds, in spite of significant exchange interactions for **1** and **3**. Such lack of ordering is probably related to the low-dimensional character of the magnetic network.

The saturation magnetization at 50 kOe reaches values of 3.13, 5.08, and 3.03 Nβ for **1**, **2**, and **3**, respectively, which corresponds to the predicted values of 3.00 Nβ for the $Cu^{II}{}_2W^V$ unit in **1** and **3**, and 5.00 Nβ for the $Cu^{II}{}_3W^V{}_2$ unit for **2** (inset Figure 8).

The magnetic properties of **1**−**3** can be interpreted in terms of Kahn's model,[53] taking into account the competition of ferro- and antiferromagnetic interaction between paramagnetic centers based on overlapping between the magnetic orbitals (Supporting

dx.doi.org/10.1021/ic200689a |*Inorg. Chem.* 2011, 50, 8808–8816

Information, Figures S4−S6).[17] The magnetic orbital of tungsten in $[W(CN)_8]^{3-}$ ion depends on the coordination geometry: $d_{x^2-y^2}$ or d_{z^2} for DD-8 or SAPR-8 environment, respectively.[54] The magnetic orbital of Cu(II) center of SPY-5 or tetragonally elongated OC-6 geometry is the $d_{x^2-y^2}$, while for TBPY-5 geometry is the d_{z^2}.[55] In the case of **1**, the magnetic orbitals for both metal centers are the $d_{x^2-y^2}$. The equatorial Cu−NC−W linkages of **1** are characterized by Cu−N−C angles of 175.0° and 175.9° and short Cu−N distances (2.002 and 2.017 Å). The axial linkages are almost linear with Cu−N−C angles of 178.5° and 176.3° with long Cu−N distances (2.188 and 2.201 Å). Very small deviation from the linearity of the Cu−N−C linkage and short Cu−N distance for the equatorial cyanido-bridges in combination with significant orthogonality of the magnetic orbitals give contribution to the ferromagnetic coupling. In the case of the axial linkages the magnetic orbitals reveal partial overlapping suggesting the small contribution of the antiferromagnetic component, partially due to the significantly longer Cu−N distances than the equatorial ones. In the case of **2**, the magnetic orbitals of metal centers are d_{z^2} (W) and $d_{x^2-y^2}$ (Cu). All of the cyanido-bridges in **2** coordinate Cu centers in the axial positions with long Cu−N distances in the range 2.375−2.669 Å and strong bending (Cu−N−C angles range from 149.7° to 165.6°). Due to the very long Cu−N coordination bonds the expected magnitude of the magnetic interaction in **2** seems to be small, and its sign (ferro- or antiferromagnetic) cannot be assigned unambiguously within the simple model of magnetic orbitals' overlapping. The situation is more clear for **3**, where the magnetic orbitals are d_{z^2}(W), $d_{x^2-y^2}$(Cu3, Cu4, Cu5), and $d_{x^2-y^2}$(Cu6). The Cu3, Cu4, and Cu5 centers have two sets of cyanido-bridges: (i) long and slightly bent axial linkages (Cu−N distances in the range 2.267−2.324 Å, Cu−N−C angles in the range 162.9−168.9°) and (ii) short and almost linear equatorial linkages (Cu−N distances in the range 1.998−2.004 Å, Cu−N−C angles in the range 170.3−176.1°). The Cu6 center has short and bent CN^- bridges coordinated in the equatorial positions (Cu−N distances 2.034 and 2.160 Å, Cu−N−C angles 174.9° and 168.9°). Furthermore, in the structure of **3** there are very long axial (Cu−O distances 2.616 and 2.724 Å) and short equatorial (Cu−O distances 1.971 and 1.986 Å) formato-bridges revealing *syn*−*anti* and *anti*−*anti* arrangements. In the inorganic−organic hybrid network of **3** the magnetic interactions are transmitted mainly by cyanido-linkages, because the formato-bridges provide small contributions to the overall magnetic interactions due to the presence of long Cu−O bonds over 2.6 Å in each of the Cu−OCO−Cu linkages.[56−58] Similarly to **1**, the equatorial bridging cyanides give a contribution to ferromagnetic coupling, contrary to axial cyanido-bridges, where antiferromagnetic interaction is preferred.

Table 3 summarizes the structural and magnetic characteristics of **1**−**3** along with other Cu(II)−NC−W(V) networks. Assemblies **1** and **2** represent 1-D chain and 2-D layer inorganic hybrid structures, respectively, while **3** forms a mixed inorganic−organic 3-D framework which is relatively rarely reported in compounds based on d-block metals and octacyanidometallates(V).

The $[Cu^{II}(Hpyr)_x(H_2O)_y]^{2+}$ units are observed in all synthesized complexes, which confirmed incorporation of $[Cu^{II}(Hpyr)_2(H_2O)_4]^{2+}$ and $[Cu^{II}(Hpyr)_4(H_2O)_2]^{2+}$ synthons with substituted water and/or pyrazole molecules for bridging cyanides. The same $[Cu^{II}(Hpyr)_x(H_2O)_y]^{2+}$ units were obtained for hydrothermal and room temperature synthesized metal complex templated octamolybdates,[59] phosphomolybdates,[60] and decavanadates.[61]

Table 3. Structure, Average Cu−N Distances, Average Cu−N−C Angles, and Magnetic Properties of 1−3 and other Cu^{II}-$[W^V(CN)_8]^{3-}$ Systems

compound	structure	topology	Cu−N_{eq}	Cu−N_{ax}	Cu−N−C_{eq}	Cu−N−C_{ax}	magnetism	ref
$Cu^{II}_2(Hpyr)_5(H_2O)[W^V(CN)_8](NO_3)\cdot H_2O$ (**1**)	1-D	vertex-sharing squares	2.010	2.195	175.5	177.4	F, θ = 17(1) K	this work
$\{Cu^{II}_5(Hpyr)_{18}[W^V(CN)_8]_4\}\cdot[Cu^{II}(Hpyr)_4(H_2O)_2]\cdot 9H_2O$ (**2**)	2-D	layer with 20 metallic units		2.507		157.6	F, θ = 2(1) K	this work
$Cu^{II}_4(Hpyr)_{10}(H_2O)[W^V(CN)_8]_2(HCOO)_2\cdot 4.5H_2O$ (**3**)	3-D	network	2.040	2.296	172.7	166.6	F, θ = 13(1) K	this work
$[Cu^{II}(cyclam)]_3[W^V(CN)_8]_2\cdot 5H_2O$	1-D	rope-ladder		2.588		153.4	F, θ = 1.54 K	8
$[Cu^{II}(tetrenH_2)][Cu^{II}(tetrenH)][W^V(CN)_8][W^{IV}(CN)_8]\cdot 2.5H_2O$	1-D	triple-ladder	1.956	2.359	169.6	149.7	AF, θ = −0.78(1) K	9
$(H_3O)\{[Cu^{II}(dien)]_4[W^V(CN)_8]\}[W^V(CN)_8]_2\cdot 6.5H_2O$	1-D	quadruple chain	1.965	2.261	163.5	144.6	F, θ = 1.74(7) K	10
$[Cu^{II}(L)]_3[W^V(CN)_8]_2\cdot 6H_2O$	2-D	honeycomb		2.593		147.0	F, θ = 3.9 K	25
$\{[Cu^{II}(L)]_3[W^V(CN)_8]_2\}\cdot[Cu^{II}(L)\cdot 2H_2O]\cdot(ClO_4)_2\cdot 2H_2O$	2-D	brick wall		2.639		146.7	F, θ = 4.1 K	24
$[Cu^{II}(tn)]_3[W^V(CN)_8]_2\cdot 3H_2O$	2-D	folded square grid with 8 and 4 metallic units	2.007	2.343	170.9	153.3	F, θ = 19.52 K, T_N = 10.7 K	14
$[Cu^{II}(pn)]_3[W^V(CN)_8]_2\cdot 3H_2O$	2-D	folded square grid with 8 and 4 metallic units	1.988	2.455	169.0	151.4	F, θ = 28.52 K, T_N = 8.1 K	14
$[\{Cu^{II}(3\text{-}CNpy)_2(H_2O)\}_2\{Cu^{II}(3\text{-}CNpy)_2(H_2O)_2\}\{W^V(CN)_8\}_2]$	2-D	folded square grid with 8 and 4 metallic units	1.976	2.247	175.2	153.5	F, T_N = 8.0 K	16
$[\{Cu^{II}(4\text{-}CNpy)_2\}_2\{Cu^{II}(4\text{-}CNpy)_2(H_2O)_2\}\{W^V(CN)_8\}_2]\cdot 6H_2O$	2-D	folded square grid with 8 and 4 metallic units	1.980	2.327	174.1	167.5	F, T_N = 4.4 K	16

dx.doi.org/10.1021/ic200689a |*Inorg. Chem.* 2011, 50, 8808–8816

Assembly **1** is unique among $Cu^{II}-[W^{V}(CN)_8]^{3-}$ systems due to 1-D vertex-sharing squares topology. Up to now three compounds with chain structure built of copper(II), organic ligand, and octacyanidometallates(V) have been reported: $[Cu^{II}(cyclam)]_3[W^{V}(CN)_8]_2\cdot 5H_2O$,[8] $[Cu^{II}(tetrenH_2)][Cu^{II}(tetrenH)][W^{V}(CN)_8][W^{IV}(CN)_8]\cdot 2.5H_2O$,[9] and $(H_3O)\{[Cu^{II}(dien)]_4[W^{V}(CN)_8]\}[W^{V}(CN)_8]_2\cdot 6.5H_2O$.[10] In the Cu(II)−NC−W(V) series, these assemblies represent topology of rope-ladder, triple-ladder, and quadruple chain, respectively, but topology of vertex-sharing squares is unique for **1**. The vertex-sharing squares topology has been observed in the other assemblies: $\{[Mn^{II}(tptz)(CH_3OH)]_2[W^{IV}(CN)_8]\cdot 2CH_3OH\}_{\infty}$,[62] $\{[Mn^{II}(bpy)(dmf)_2]_2[Mo^{IV}(CN)_8]\cdot 1.5H_2O\}_n$,[63] and $[\{Mn^{II}(phen)_2\}_6\{W^{IV}(CN)_8\}_3(H_2O)_2]\cdot 21H_2O$.[64] However, these compounds reveal different magnetic properties than **1**. For $Mn^{II}-[M^{IV}(CN)_8]^{4-}$ (M = Mo, W) systems antiferromagnetic coupling between the Mn^{II} ions through the diamagnetic NC−M^{IV}−CN bridges has been reported while for **1** we have observed ferromagnetic coupling through Cu^{II}−NC−W^{V} bridges with the Weiss constant θ = 17(1) K. The similar weak ferromagnetic interaction was observed for $[Cu^{II}(cyclam)]_3[W^{V}(CN)_8]_2\cdot 5H_2O$ and $(H_3O)\{[Cu^{II}(dien)]_4[W^{V}(CN)_8]\}[W^{V}(CN)_8]_2\cdot 6.5H_2O$.

Compound **2** is the first example of 2-D layer structure with a $[Cu^{II}(Hpyr)_2(H_2O)_4]^{2+}$ complex inside the large coordination spaces. The same effect of charge compensation with a non-bridged moiety was observed for $[Cu(en)_2(H_2O)_2]^{2+}$ complex in 1-D chain of $[Cu^{II}(en)_2][Cu^{II}_{0.5}(en)][Cu^{II}_{0.5}(en)(H_2O)][Mo^{IV}(CN)_8]\cdot 4H_2O$,[65] $[Cu^{II}(L)\cdot 2H_2O]^{2+}$ in 2-D layer of $\{[Cu^{II}(L)]_3[W^{V}(CN)_8]_2\}\cdot[Cu^{II}(L)\cdot 2H_2O]\cdot(ClO_4)_2\cdot 2H_2O$,[24] and $[Nd^{III}(H_2O)_8]^{3+}$ hydrate ion in 3-D network of $[\{Nd^{III}(CH_3OH)_4Mo^{IV}(CN)_8\}_3]^{3-}\cdot[Nd^{III}(H_2O)_8]^{3+}\cdot 8CH_3OH$.[66] Magnetic properties of **2** suggested weak ferromagnetic interaction, which is typical for $Cu^{II}-[W^{V}(CN)_8]^{3-}$ systems.

The structure of **3** is extraordinary because, to the best of our knowledge, it is the first complex based on cyanido- and formato-bridges revealing mixed inorganic−organic framework (I^1O^2). Furthermore, we observe the presence of structural subunits consisting of 1-D vertex-sharing squares chains, which are linked together through formate ions. The other cyanido-bridged system revealing the I^1O^2 framework reported so far is $\{Mn^{II}_9(dpe)_5[W^{V}(CN)_8]_6(CH_3OH)_{10}\}\cdot 14CH_3OH$.[67] Coordination polymer **3** exhibits ferromagnetic coupling through Cu^{II}−NC−W^{V} bridges with the Weiss constant value (θ) of 13(1) K.

CONCLUSIONS

As a part of our program aimed at the construction of magnetic of $Cu^{II}-[W^{V}(CN)_8]^{3-}$ inorganic−organic hybrid coordination polymers we have found that the challenging synthesis of novel assemblies is susceptible to the influence of microwave irradiation. To the best of our knowledge, we demonstrate the first examples of molecular systems based on octacyanidometallates obtained as the result of the microwave-assisted protocol.

Moreover, we observe that products of microwave synthesis are heavily dependent on the type of compounds used in synthesis, and these assemblies are strongly different in comparison to $Cu^{II}-[W^{V}(CN)_8]^{3-}$ systems synthesized at ambient conditions. Compound **1** represents the 1-D vertex-sharing squares topology which has been only observed for $Mn^{II}-[M^{IV}(CN)_8]^{4-}$ (M = Mo, W) systems. The same structural motif is obtained for assembly **3**, but in this case the structure is extended by formato-bridges to the 3-D mixed inorganic−organic framework. Assembly **2** represents the 2-D layer with extraordinary large $Cu_{10}W_{10}$ windows with $[Cu^{II}(Hpyr)_2(H_2O)_4]^{2+}$ complexes inside.

Results of magnetic measurements of **1** and **3** are almost identical which indicates that formato-bridges in **3** have a weak influence on the magnetic properties. Magnetic properties of **2** are similar to results for other $Cu^{II}-[W^{V}(CN)_8]^{3-}$ systems with 6 metallic units of honeycomb and brick wall topology.[24,25]

Studies on the structure and magnetic properties of the green primary product (**A**) formed without microwave irradiation as well as the research to improve the scope and utility of the microwave-assisted construction of molecular systems based on octacyanidometallates are underway in our laboratory.

ASSOCIATED CONTENT

Supporting Information. Interpretation of IR spectra of Hpyr, green precipitate (**A**), and **1**−**3**; SHAPE parameters for Cu and W centers; and the qualitative representation of magnetic orbitals in **1**−**3**. Crystal data in CIF format. This material is available free of charge via the Internet at http://pubs.acs.org.

AUTHOR INFORMATION

Corresponding Author
*E-mail: barbara.sieklucka@uj.edu.pl.

ACKNOWLEDGMENT

This work was partially supported by the Polish Ministry of Science and Higher Education within Research Projects N N204 153536 and by the International PhD-studies Programme at the Faculty of Chemistry Jagiellonian University within the Foundation for Polish Science MPD Programme cofinanced by the EU European Regional Development Fund. The research was partially carried out with the equipment purchased thanks to the financial support of the European Regional Development Fund in the framework of the Polish Innovation Economy Operational Program (Contract POIG.02.01.00-12-023/08).

REFERENCES

(1) Cheetham, A. K.; Rao, C. N. R.; Feller, R. K. *Chem. Commun.* **2006**, 4780–4795.
(2) Férey, G. *Chem. Soc. Rev.* **2008**, *37*, 191–214.
(3) Rao, C. N. R.; Cheetham, A. K.; Thirumurugan, A. *J. Phys.: Condens. Matter* **2008**, *20*, 083202.
(4) Sieklucka, B.; Podgajny, R.; Korzeniak, T.; Nowicka, B.; Pinkowicz, D.; Kozieł, M. *Eur. J. Inorg. Chem.* **2011**, *3*, 305–326.
(5) Wang, J.; Zhang, Z.-Ch.; Wang, H.-S.; Kang, L.-Ch.; Zhou, H.-B.; Song, Y.; You, X.-Z. *Inorg. Chem.* **2010**, *49*, 3101–3103.
(6) Korzeniak, T.; Desplanches, C.; Podgajny, R.; Giménez-Saiz, C.; Stadnicka, K.; Rams, M.; Sieklucka, B. *Inorg. Chem.* **2009**, *48*, 2865–2872.
(7) Kou, H.-Z.; Zhou, B. C.; Si, Sh.-F.; Wang, R.-J. *Eur. J. Inorg. Chem.* **2004**, 401–408.
(8) Lim, J. H.; You, Y. S.; Yoo, H. S.; Yoon, J. H.; Kim, J. I.; Koh, E. K.; Hong, Ch. S. *Inorg. Chem.* **2007**, *46*, 10578–10586.
(9) Podgajny, R.; Korzeniak, T.; Stadnicka, K.; Dromzée, Y.; Alcock, N. W.; Errington, W.; Kruczała, K.; Bałanda, M.; Kemp, T. J.; Verdaguer, M.; Sieklucka, B. *Dalton Trans.* **2003**, 3458–3468.
(10) Podgajny, R.; Pełka, R.; Desplanches, C.; Ducasse, L.; Nitek, W.; Korzeniak, T.; Stefanczyk, O.; Rams, M.; Sieklucka, B.; Verdaguer, M. *Inorg. Chem.* **2011**, 3213–3222.
(11) Kaneko, S.; Tsunobuchi, Y.; Sakurai, Sh.; Ohkoshi, S. *Chem. Phys. Lett.* **2007**, *446*, 292–296.

(12) Wang, Y.; Wang, T.-W.; Xiao, H.-P.; Li, Y.-Z.; Song, Y.; You, X.-Z. *Chem.—Eur. J.* **2009**, *15*, 7648–7655.
(13) Higashikawa, H.; Okuda, K.; Kishine, J.; Masuhara, N.; Inoue, K. *Chem. Lett.* **2007**, *36*, 1022–1023.
(14) Li, D.-F.; Zheng, L.-M.; Wang, X.-Y.; Huang, J.; Gao, S.; Tang, W.-X. *Chem. Mater.* **2003**, *15*, 2094–2098.
(15) Li, D.-F.; Gao, S.; Zheng, L.-M.; Yu, K.-B.; Tang, W.-X. *New. J. Chem.* **2002**, *26*, 1190–1195.
(16) Ohkoshi, S.; Arimoto, Y.; Hozumi, T.; Seino, H.; Mizobe, Y.; Hashimoto, K. *Chem. Commun.* **2003**, 2772–2773.
(17) Korzeniak, T.; Stadnicka, K.; Rams, M.; Sieklucka, B. *Inorg. Chem.* **2004**, *43*, 4811–4813.
(18) Imoto, K.; Kaneko, S.; Tsunobuchi, Y.; Nakabayashi, K.; Ohkoshi, S. *Acta Crystallogr.* **2010**, *E66*, m403–m404.
(19) Korzeniak, T.; Podgajny, R.; Alcock, N. W.; Lewiński, K.; Bałanda, M.; Wasiutyński, T.; Sieklucka, B. *Polyhedron* **2003**, *22*, 2183–2190.
(20) Podgajny, R.; Chmel, N. P.; Bałanda, M.; Tracz, P.; Gaweł, B.; Zając, D.; Sikora, M.; Kapusta, Cz.; Łasocha, W.; Wasiutyński, T.; Sieklucka, B. *J. Mater. Chem.* **2007**, *17*, 3308–3314.
(21) Podgajny, R.; Korzeniak, T.; Bałanda, M.; Wasiutyński, T.; Errington, W.; Kemp, T. J.; Alcock, N. W.; Sieklucka, B. *Chem. Commun.* **2002**, 1138–1139.
(22) Korzeniak, T.; Stadnicka, K.; Pełka, R.; Bałanda, M.; Tomala, K.; Kowalski, K.; Sieklucka, B. *Chem. Commun.* **2005**, 2939–2941.
(23) Lim, J. H.; Kang, J. S.; Kim, H. Ch.; Koh, E. K.; Hong, Ch. S. *Inorg. Chem.* **2006**, *45*, 7821–7827.
(24) Yuan, A.-H.; Liu, W.-Y.; Zhou, H.; Chen, Y.-Y.; Shen, X.-P. *J. Mol. Struct.* **2009**, *919*, 356–360.
(25) Yoon, Y. S.; Lim, J. H.; Kim, H. Ch.; Hong, Ch. S. *Inorg. Chem.* **2005**, *44*, 7063–7069.
(26) Ohkoshi, S.; Machida, N.; Zhong, Z. J.; Hashimoto, K. *Synth. Met.* **2001**, *122*, 523–527.
(27) Garde, R.; Desplanches, C.; Bleuzen, A.; Veillet, P.; Verdaguer, M. *Mol. Cryst. Mol. Liq. Cryst.* **1999**, *334*, 587.
(28) Li, D.-F.; Gao, S.; Zheng, L.-M.; Sun, W.-Y.; Okamura, T.; Ueyama, N.; Tang, W.-X. *New J. Chem.* **2002**, *26*, 485–489.
(29) Tsunobuchi, Y.; Hashimoto, K.; Shiro, M.; Hozumi, T.; Ohkoshi, S. *Chem. Lett.* **2007**, *36*, 1464–1465.
(30) Ohkoshi, S.; Tsunobuchi, Y.; Takahashi, H.; Hozumi, T.; Shiro, M.; Hashimoto, K. *J. Am. Chem. Soc.* **2007**, *129*, 3084–3085.
(31) Kaneko, S.; Tsunobuchi, Y.; Nakabayashi, K.; Ohkoshi, S. *Polyhedron* **2009**, *28*, 1893–1797.
(32) Kaneko, S.; Tsunobuchi, Y.; Nakabayashi, K.; Ohkoshi, S. *Acta Crystallogr.* **2008**, *E64*, m1442–m1443.
(33) Chen, F.-T.; Li, D.-F.; Gao, S.; Wang, X.-Y.; Li, Y.-Z.; Zheng, L.-M.; Tang, W.-X. *Dalton Trans.* **2003**, 3283–3287.
(34) Casarin, M.; Corvaja, C.; Di Nicola, C.; Falcomer, D.; Franco, L.; Monari, M.; Pandolfo, L.; Pettinari, C.; Piccinelli, F. *Inorg. Chem.* **2005**, *44*, 6265–6276.
(35) Angaroni, M.; Ardizzoia, G. A.; Beringhelli, T.; La Monica, G.; Gatteschi, D.; Masciocchi, N.; Moret, M. *J. Chem. Soc., Dalton Trans.* **1990**, 3305–3309.
(36) Cingolani, A.; Galli, S.; Masciocchi, N.; Pandolfo, L.; Pettinari, C.; Sironi, A. *J. Am. Chem. Soc.* **2005**, *127*, 6144–6145.
(37) Otieno, T.; Blanton, J. R.; Hatfield, M. J.; Asher, S. L.; Parkin, S. *Acta Crystallogr.* **2002**, *C58*, m182–m185.
(38) Xing, Y.-H.; Han, J.; Zhang, B.-L.; Zhang, X.-J.; Zhang, Y.-H.; Zhou, G.-H. *Acta Crystallogr.* **2006**, m3354–m3356.
(39) Goslar, J.; Sczaniecki, P. B.; Strawiak, M. M.; Mroziński, J. *Transition Met. Chem.* **1988**, *13*, 81–86.
(40) Shen, W.-Z.; Yi, L.; Cheng, P.; Yan, S.-P.; Liao, D.-Z.; Jiang, Z.-H. *Inorg. Chem. Commun.* **2004**, *7*, 819–822.
(41) Adams, C. J.; Kurawa, M. A.; Orpen, A. G. *Dalton Trans.* **2010**, *39*, 6974–6984.
(42) Samotus, A. *Pol. J. Chem.* **1973**, *47*, 653.
(43) Bok, L. D. C.; Leipoldt, J. G.; Basson, S. S. *Z. Anorg. Allg. Chem.* **1975**, *415*, 81–83.
(44) McArdle, P. *J. Appl. Crystallogr.* **1996**, *29*, 306.
(45) Altomare, A.; Burla, M. C.; Camalli, M.; Cascarano, G. L.; Giacovazzo, C.; Guagliardi, A.; Moliterni, A. G. G.; Polidori, G.; Spagna, R. *J. Appl. Crystallogr.* **1999**, *32*, 115–119.
(46) Sheldrick, G. M. *Acta Crystallogr.* **2008**, *A64*, 112–122.
(47) Farrugia, L. J. *J. Appl. Crystallogr.* **1999**, *32*, 837–838.
(48) Macrae, C. F.; Edgington, P. R.; McCabe, P.; Pidcock, E.; Shields, G. P.; Taylor, R.; Towler, M.; van de Streek, J. *J. Appl. Crystallogr.* **2006**, *39*, 453–457.
(49) Llunell, M.; Casanova, D.; Cirera, J.; Alemany, M. P.; Alvarez, S. *SHAPE, v.2.0; Program for the Stereochemical Analysis of Molecular Fragments by Means of Continuous Shape Measures and Associated Tools*; Departament de Química Física, Departament de Química Inorgànica, and Institut de Química Teòrica i Computacional, Universitat de Barcelona: Barcelona, Spain, 2010.
(50) Przychodzeń, P.; Korzeniak, T.; Podgajny, R.; Sieklucka, B. *Coord. Chem. Rev.* **2006**, *250*, 2234–2260.
(51) Manson, J. L.; Lancaster, T.; Schluter, J. A.; Blundell, S. J.; Brooks, M. L.; Pratt, F. L.; Nyger, C. L.; Koo, H.-J.; Dai, D.; Whangbo, M.-H. *Inorg. Chem.* **2007**, *46*, 213–220.
(52) Valach, F. *Polyhedron* **1999**, *18*, 699–706.
(53) Kahn, O. *Molecular Magnetism*; VCH Publishers: New York, 1993; Chapter 8.4.2.
(54) Visinescu, D.; Desplanches, C.; Imaz, I.; Bahers, V.; Pradhan, R.; Villamena, F. A.; Guionneau, P.; Sutter, J.-P. *J. Am. Chem. Soc.* **2006**, *128*, 10202–10212.
(55) Gispert, J. R. *Coordination Chemistry*; Wiley-VCH: Weinheim, 2008; Chapter 3.
(56) Rodríguez-Fortea, A.; Alemany, P.; Alvarez, S.; Ruiz, E. *Chem.—Eur. J.* **2001**, *7*, 627–637.
(57) Christou, G.; Perlepes, S. P.; Libby, E.; Folting, K.; Huffman, J. C.; Webb, R. J.; Hendrickson, D. N. *Inorg. Chem.* **1990**, *29*, 3657–3666.
(58) Colacio, E.; Ghazi, M.; Kivekäs, R.; Moreno, J. M. *Inorg. Chem.* **2000**, *39*, 2882–2890.
(59) Pavani, K.; Lofland, S. E.; Ramanujachary, K. V.; Ramanan, A. *Eur. J. Inorg. Chem.* **2007**, 568–578.
(60) Thomas, J.; Ramanan, A. *Cryst. Growth Des.* **2008**, *8*, 3390–3400.
(61) Thomas, J.; Agarwal, M.; Ramanan, A.; Chernova, N.; Whittingham, M. S. *CrystEngComm* **2009**, *11*, 625–631.
(62) Zhao, H.; Shatruk, M.; Prosvirin, A. V.; Dunbar, K. R. *Chem.—Eur. J.* **2007**, *13*, 6573–6589.
(63) Ma, S.-L.; Ma, Y.; Ren, S.; Yan, S.-P.; Liao, D.-Z. *Struct. Chem.* **2008**, *19*, 329–338.
(64) Venkatakrishnan, T. S.; Rajamani, R.; Ramasesha, S.; Sutter, J.-P. *Inorg. Chem.* **2007**, *46*, 9569–9574.
(65) Zhang, W.; Sun, H.-L.; Sato, O. *Dalton Trans.* **2011**, *40*, 2735–2743.
(66) Wang, Z.-X.; Shen, X.-F.; Wang, J.; Zhang, Y.-Z.; Nfor, E. N.; Song, Y.; Ohkoshi, S.; Hashimoto, K.; You, X.-Z. *Angew. Chem., Int. Ed.* **2006**, *45*, 3287–3291.
(67) Podgajny, R.; Chorazy, Sz.; Nitek, W.; Rams, M.; Bałanda, M.; Sieklucka, B. *Cryst. Growth Des.* **2010**, *10*, 4693–4696.